Growth-dependent changes in elemental stoichiometry and macromolecular allocation in the coccolithophore *Emiliania huxleyi* under different environmental conditions

Yong Zhang,[1,2]* **Zhengke Li,**[2] **Kai G. Schulz,**[3] **Yingyu Hu,**[2] **Andrew J. Irwin,**[4] **Zoe V. Finkel**[2]

[1]College of Environmental Science and Engineering, and Fujian Key Laboratory of Pollution Control and Resource Recycling, Fujian Normal University, Fuzhou, China
[2]Department of Oceanography, Dalhousie University, Halifax, Nova Scotia, Canada
[3]Centre for Coastal Biogeochemistry, School of Science, Environment and Engineering, Southern Cross University, Lismore, New South Wales, Australia
[4]Department of Mathematics & Statistics, Dalhousie University, Halifax, Nova Scotia, Canada

Abstract

The growth rate hypothesis (GRH) posits an increase in ribosomal ribonucleic acid (RNA) content, and therefore cellular phosphorus (P), with increasing growth rate. There is evidence that the GRH may not apply to phytoplankton under all conditions. Here, we experimentally controlled four conditions (light, temperature, pH, and CO_2) to alter the growth rate of *Emiliania huxleyi*, a biogeochemically important coccolithophorid, and monitored changes in RNA, protein, and carbohydrate content. We show that an increase in growth rate caused by increasing light, pH, and CO_2 resulted in increased RNA per unit of organic carbon (RNA : POC), but that increasing temperature, leading to increase of growth rate, resulted in a decrease in RNA : POC. Protein per unit of organic carbon (protein : POC) increased in our increased temperature, pH, and CO_2 treatments that increased growth rate, but there was little change in protein : POC in our light treatment despite it inducing the same increase in growth rate. Carbohydrate per unit of organic carbon (Carbohydrate : POC) increased with growth rate under increased light and CO_2 but did not vary significantly in the temperature or pH treatments. These results indicate that physiological acclimation to specific environmental conditions can lead to contrasting patterns in RNA, protein, and carbohydrate composition and therefore contrasting changes in carbon : nitrogen : phosphorus ratios with growth rate in *E. huxleyi*.

Alfred Redfield found that the molar ratio of carbon (C), nitrogen (N), and phosphorus (P) of marine plankton is often approximately 106 : 16 : 1 (Redfield 1958). There is increasing recognition that the C : N : P of plankton varies widely across regions and seasons and is associated with differences in community composition, nutrient supply rates, and environmental conditions (Finkel et al. 2010, 2016; Martiny et al. 2013, 2016). The C : N : P of plankton affects the C, N, and P cycles in the ocean (Redfield 1958; Weber and Deutsch 2010). Thus, quantifying the impact of marine environmental drivers on

the elemental stoichiometry of key plankton groups will improve our ability to model the biogeochemical cycles of C, N, and P (Arrigo 2005; Daines et al. 2014; Moreno and Martiny 2018).

The growth rate hypothesis (GRH) posits that growth rate will regulate elemental composition through shifts in cellular protein and RNA content. Specifically, Elser et al. (2000) propose that higher growth rates require a larger investment in P-rich ribosomes (RNA) to increase protein synthesis rates. As a consequence, increases in growth rate are expected to be associated with higher RNA : POC, RNA : protein, and therefore lower N : P content (Elser et al. 2000; Finkel et al. 2010; Moreno and Martiny 2018). The GRH and resulting impact on C : N : P assumes that ribosome activity per unit of ribosomal RNA (rRNA) is relatively constant and P allocated to rRNA constitutes the majority of the cellular P content (Elser et al. 2003; Flynn et al. 2010). The applicability of the GRH to phytoplankton has been questioned (Flynn et al. 2010; Garcia et al. 2016; Moreno and Martiny 2018). One of the reasons that growth rate may not be correlated with N : P is that

*Correspondence: yongzhang@fjnu.edu.cn

phytoplankton are capable of luxury P consumption and can store large amounts of P (Dyhrman et al. 2006; Orchard et al. 2010; Diaz et al. 2016). In addition, individual environmental drivers may uniquely alter macromolecular allocation (protein, carbohydrate, RNA, pigments) and C : N : P in phytoplankton (Harris et al. 2009; Giordano et al. 2015; Liefer et al. 2019). Much of the work that supports the GRH was conducted on freshwater organisms and growth was often controlled by phosphorus, which will have a direct impact on cellular P content and P-rich cellular machinery (Elser et al. 2003; Nicklisch and Steinberg 2009; Flynn et al. 2010). There are few studies comparing the applicability of the GRH in phytoplankton under a range of environmental conditions (Giordano et al. 2015; Garcia et al. 2016) such as irradiance, temperature, carbon dioxide (CO_2) concentration, and pH.

Coccolithophores are biogeochemically important constituents of phytoplankton communities that produce both particulate organic carbon (POC) via photosynthesis and particulate inorganic carbon (PIC) through calcification (Rost and Riebesell 2004). Within subtropical gyres coccolithophores may contribute 20% or more to total organic carbon fixation (Poulton et al. 2007), and about 50% of $CaCO_3$ export to tropical and higher-latitude sediments (Broecker and Clark 2009), and hence they play an important role in the marine biological C pump and the biogeochemical cycling of carbon. The cosmopolitan coccolithophore *Emiliania huxleyi* is able to form massive blooms in temperate and subpolar waters (Iida et al. 2012; Kondrik et al. 2019). Therefore, it is of interest to improve our biochemical understanding of how the biogeographically dominant *E. huxleyi*, alter both carbon fixation and C : N : P under a range of environmental conditions (Riebesell and Tortell 2011; Rivero-Calle et al. 2015; Krumhardt et al. 2017).

Carbon dioxide concentration and pH appear to have their own unique physiological effects on coccolithophores; CO_2 concentration mainly influences photosynthetic carbon fixation and carbohydrate synthesis, while pH alters cellular pH homeostasis and ion balance, with downstream impacts on enzyme activity and C, N, and P metabolism (Hinga 2002; Taylor et al. 2011; Bach et al. 2013). There is not enough data available to fully evaluate how CO_2 or pH will alter RNA and protein content and shift C : N : P in coccolithophores (Engel et al. 2014; Olson et al. 2017) (Table S1). Increasing irradiance, below supersaturating levels, generally causes an increase in carbon storage and downregulation of light harvesting pigment–protein complexes in phytoplankton, often leading to higher C : N and lower N : P with increasing growth rates (Leonardos and Geider 2005; Jin et al. 2017; Feng et al. 2018) (Table S1). In contrast, in response to lowered temperature, organisms sometimes increase cellular RNA content, resulting in lower C : P and N : P (Feng et al. 2018; Wang et al. 2019). To improve our understanding of how environmental conditions influence macromolecular and elemental composition and to test the GRH in the coccolithophore *E. huxleyi* over a range of conditions we quantify how C : N : P, RNA, and protein content vary with growth rate at 28, 45, and 280 μmol photons m^{-2} s^{-1}; at 11.0°C, 14.5°C, and 22.0°C; at pH 6.70, 7.40, and 8.04; and at 2.70, 6.40, and 41.10 Pa.

Methods

Experimental setup

E. huxleyi strain RCC1266 (morphotype A), originally isolated from shelf waters around Ireland (49°30′N, 10°30′ W), was obtained from the Roscoff algal culture collection. In the control treatment, *E. huxleyi* cells were maintained in 280 μmol photons m^{-2} s^{-1} under a 12 h : 12 h light : dark cycle (light period: 07:00 to 19:00 h), 22.0°C, pH_{Total} (total scale) 8.04, and 41.10 Pa (1 Pa $\approx$ 10 μatm) pCO_2 in semicontinuous cultures. We defined the maximum growth rate (μ_{max}) as the steady-state exponential growth rate under the control conditions in this experiment. Experimental treatments include two subsaturating irradiances (28 and 45 μmol photons m^{-2} s^{-1}), two lower suboptimal temperatures (11.0°C and 14.5°C), two lower pH (6.70 and 7.40), and two lower CO_2 concentrations (2.70 and 6.40 Pa), chosen to reduce growth rate to approximately $\frac{3}{4}\mu_{max}$ and $\frac{1}{2}\mu_{max}$ relative to the control (*see* Table 1 for a summary). Please note that the experimental conditions in the control treatment and the maximum growth rate are the same for all treatments. During pre-experiments, we investigated the growth response of *E. huxleyi* to a broad range of light intensities, temperatures, pH values, and CO_2 concentrations. Changing one condition at a time, we found that growth rates were close to $\frac{3}{4}\mu_{max}$ at 45 μmol photons m^{-2} s^{-1}, 14.5°C, pH 7.40, and 6.40 Pa, and close to $\frac{1}{2}\mu_{max}$ at 28 μmol photons m^{-2} s^{-1}, 11.0°C, pH 6.70, and 2.70 Pa. The artificial seawater (ASW) media was prepared according to Berges et al. (2001) without the addition of $NaHCO_3$, with a salinity of 33 psu. The dissolved inorganic carbon (DIC)–free ASW media was enriched with 100 μmol L^{-1} NO_3^-, 6.25 μmol L^{-1} PO_4^{3-}, 4.24 μmol L^{-1} SiO_3^{2-}, L1/4 concentrations for trace elements, and f/8 concentrations for vitamins (Guillard and Ryther 1962; Guillard and Hargraves 1993). The carbonate chemistry of the enriched media was adjusted by adding 1.18 mol kg^{-1} Na_2CO_3 and 2.00 mol kg^{-1} hydrochloric acid (HCl) to achieve target pH_{Total} (total scale) and CO_2 levels (see below for more detail).

In the light and temperature treatments (four replicates), carbonate chemistry was preadjusted by stepwise additions of Na_2CO_3 and HCl. For the pH 7.40 and 6.70 treatments, calculated concentrations of Na_2CO_3 were added into the enriched ASW to maintain similar pCO_2 levels (about 41.00 Pa). Seawater pH was then adjusted to 7.40 or 6.70 by adding 5 mmol L^{-1} of 2-[-4-(2-hydroxyethyl)-1-piperazinyl]-ethanesulfonic acid (HEPES). For the 6.40 and 2.70 Pa CO_2 treatments, calculated amounts of Na_2CO_3 were added to the enriched ASW (to reach the predescribed growth rates), and pH was adjusted to 8.04 by adding 5 mmol L^{-1} HEPES. There were four replicates at pH 7.40 and

Table 1. Measured light intensity, temperature, carbonate chemistry parameters at the start and end of the incubation, and changes in carbonate chemistry parameters during the incubation. Data are one replicate at the start of incubation and means ± SD of four replicates at the end of the incubation. L280, L45, L28, T14.5, T11.0, pH 7.40, pH 6.70, C6.40, and C2.70 indicate that samples are, respectively, cultured under 280, 45, or 28 μmol photons m^{-2} s^{-1}, under 14.5°C or 11.0°C, under pH 7.40 or 6.70, under 6.40 or 2.70 Pa CO$_2$ conditions.

Treatment			Light (μmol photons m^{-2} s^{-1})	Temperature (°C)	pCO$_2$ (Pa)	pH (total scale)	TA (μmol kg^{-1})	DIC (μmol kg^{-1})	HCO$_3^-$ (μmol kg^{-1})	CO$_3^-$ (μmol kg^{-1})	CO$_2$ (μmol kg^{-1})
Control	L280	Start	280	22.0	41.05	8.04	2278	2002	1791	198.70	12.70
		End			32.62±0.62	8.11±0.01	2191±1	1885±4	1660±6	214.91±2.58	10.09±0.19
		Change			20.53%	6.69%	3.84%	5.86%	7.31%	8.13%	20.53%
Light	L45	Start	45	22.0	41.05	8.04	2278	2002	1791	198.70	12.70
		End			34.59±0.5	8.10±0.01	2226±4	1925±4	1701±5	212.95±1.93	10.70±0.20
		Change			15.73%	5.22%	2.30%	3.85%	4.99%	7.14%	15.73%
	L28	Start	28	22.0	41.05	8.04	2278	2002	1791	198.70	12.70
		End			31.99±0.7	8.11±0.01	2198±2	1886±5	1658±6	218.65±2.91	9.89±0.20
		Change			22.06%	7.49%	3.53%	5.77%	7.41%	10.01%	22.06%
Temperature	T14.5	Start	280	14.5	42.42	8.03	2277	2067	1899	152.10	16.30
		End			32.45±1.26	8.10±0.01	2111±1	1879±7	1706±10	160.57±4.24	12.43±0.48
		Change			23.51%	7.00%	7.27%	9.11%	10.16%	5.57%	23.51%
	T11.0	Start	280	11.0	41.03	8.04	2279	2090	1936	137.00	17.60
		End			35.53±1.01	8.10±0.01	2293±4	2078±6	1909±8	153.93±3.07	15.20±0.43
		Change			13.40%	5.66%	6.30%	0.57%	1.37%	12.38%	13.40%
pH	pH 7.40	Start	280	22.0	40.80	7.40		431	408	10.40	12.60
		End			32.30±1.20	7.40±0.01		344±10	326±10	8.40±0.30	9.97±0.40
		Change			20.91%	0.50%		20.01%	20.00%	19.06%	20.91%
	pH 6.70	Start	280	22.0	41.30	6.70		96	82	0.40	12.80
		End			24.50±0.60	6.72±0.01		58±2	51±2	0.27±0.01	7.60±0.18
		Change			40.73%	1.50%		38.91%	38.63%	36.47%	40.73%
CO$_2$	C6.40	Start	280	22.0	6.40	8.04		312	279	31.00	2.00
		End			4.60±0.10	8.08±0.01		248±4	220±4	26.90±0.50	1.40±0.04
		Change			28.55%	4.25%		20.45%	21.21%	13.11%	28.55%
	C2.70	Start	280	22.0	2.70	8.04		130	116	12.90	0.80
		End			1.80±0.10	8.08±0.01		98±2	87±1	10.60±0.30	0.57±0.00
		Change			31.07%	3.75%		24.21%	24.85%	18.05%	31.07%

6.40 Pa CO_2 treatments, and eight replicates at pH 6.70 and 2.70 Pa CO_2 treatments. Under the light, temperature, and pH treatments, the seawater was placed in the incubator at the appropriate experimental temperature and bubbled for 24 h with filter-sterilized air pumped from the room. The dry air was humidified with Milli-Q water prior to the aeration to minimize evaporation. Under the CO_2 treatments, the ASW was not bubbled but was put into the incubator at 22.0°C for 24 h prior to inoculation.

After measuring pH_{Total} the media was filtered (0.22 μm pore size, Polycap 75 AS, Whatman) and carefully pumped into autoclaved 250 mL (for total alkalinity [TA] measurements under the light and temperature treatments, for DIC measurements under the pH and CO_2 treatments), 2300 mL (for pre-experimental cultures), and 4630 mL (for experimental cultures) polycarbonate (PC) bottles with no headspace to minimize gas exchange. The volumes of culture inoculum were calculated to match the volume of media taken out from the bottles before inoculation. Cultures were diluted every 3 or 4 d under the light and temperature treatments and every 2 d under the pH and CO_2 treatments, and maintained in exponential growth for 16 d at 28 μmol photons m^{-2} s^{-1}, 11.0°C, pH 6.70, and 2.70 Pa CO_2, and for 12 d at 45 μmol photons m^{-2} s^{-1}, 14.5°C, pH 7.40, and 6.40 Pa CO_2 with a minimum of 16 generations. The dilution volumes were about 4340 mL under the control, 28 μmol photons m^{-2} s^{-1} and 11.0°C treatments, 4390 mL under the 45 μmol photons m^{-2} s^{-1} and 14.5°C treatments, 4140 mL under the pH 7.40 and 6.40 Pa CO_2 treatments, and 3630 mL under the pH 6.70 and 2.70 Pa CO_2 treatments. Initial cell density was about 5000 cells mL^{-1} at all treatments and final cell densities were 65,000–100,000 cells mL^{-1} under the light and temperature treatments and 23,000–62,000 cells mL^{-1} under the pH and CO_2 treatments (Fig. S1). Cultures were harvested 2 d after dilution in the control, the pH and CO_2 treatments, 3 d after dilution in the 45 μmol photons m^{-2} s^{-1} light treatment and 14.5°C temperature treatment, and 4 d after dilution in the 28 μmol photons m^{-2} s^{-1} irradiance and 11.0°C temperature treatments. Culture bottles were mixed three times per day at 09:00 h, 13:00 h, and 18:00 h. In the last day of the incubation at each light, temperature, pH, and CO_2 conditions, subsamples were taken for measurements of TA or DIC, pH_{Total}, cell concentrations, cellular contents of total particulate carbon (TPC), POC, nitrogen (PON) and phosphorus (POP), protein, RNA, carbohydrate, and pigment.

Carbonate chemistry measurements

Samples for determinations of pH_{Total} (total scale), TA, and DIC were syringe-filtered (0.22 μm pore size, Millex-GV filter), and the bottles were filled from bottom to top with overflow and closed immediately without a headspace. The pH_{Total} was measured immediately under the incubation temperatures using a pH meter which was calibrated with buffers (Tris•HCl, Hanna) at pH 4.01, 7.00 and 10.00. TA and DIC samples (250 mL) were treated with 100 μL saturated $HgCl_2$ solution

and stored in the dark at 4.0°C. TA and DIC samples were analyzed by potentiometric and coulometric titration, respectively, using a VINDTA 3C (Marianda) according to Dickson et al. (2007). Carbonate chemistry parameters were calculated using the CO2SYS program of Pierrot et al. (2006) with equilibrium constants of Roy et al. (1993). Initial CO_2 levels ranged from 40.80 to 42.42 Pa under the light, temperature, and pH treatments, and were 6.40 and 2.70 Pa under the CO_2 treatments (Table 1). Initial pH values were 8.03 or 8.04 under the light, temperature, and CO_2 treatments, and were 7.40 and 6.70 under the pH treatments. During the experiment, DIC concentrations decreased due to organismal activity by, on average, 0.57% to 38.91% under the various light, temperature, pH, and CO_2 treatments (Table 1). TA concentrations decreased by 2.30% to 7.27% under the light and temperature treatments, respectively. Correspondingly, CO_2 levels in the culture decreased by, on average, 13.40% to 40.73% under the various light, temperature, pH and CO_2 treatments. pH_{Total} values increased by less than 0.1 unit under all treatments (Table 1). The small changes in pH value under the pH and CO_2 treatments are due to HEPES buffering.

Cell density measurements

Twenty-five milliliter samples were taken daily at 13:00 h and fresh media with the same carbonate chemistry as in the initial treatment conditions were added as top-up. Cell density was measured using a Z2 Coulter Particle Count and Size Analyzer (Beckman Coulter). A flow cytometry (BD Accuri C6, MI) was used to measure cell density in the pH 6.70 and 2.70 Pa CO_2 treatments because coccosphere volumes became too small to reliably measure in the Z2 Particle Counter. Variation in measured cell concentrations was ± 2% between the two methods. Growth rate (μ) was calculated for each replicate according to the equation: $\mu = (\ln N_t - \ln N_0)/t$, where N_t and N_0 refer to the cell concentrations in the last day and beginning of the experiment, respectively, and t was the growth period in days.

Elemental and macromolecular harvesting

After mixing, samples for determinations of TPC (250 mL), POC and PON (300 mL), POP (250 mL), carbohydrate (800 mL), chlorophyll *a* (Chl *a*), and carotenoids (100 mL) were obtained by filtering onto precombusted GF/F filters (at 450.0°C for 6 h, Whatman) 7 h after the onset of the light period (at 14:00 h). Samples for determination of protein (600 mL) and RNA (800 mL) were filtered onto PC filters (25 mm diameter, 0.6 μm pore size, Nuclepore, Whatman) also at 14:00 h. Elemental and macromolecular composition was sampled only at the end of the incubations. Under the pH 6.70 and 2.70 Pa CO_2 treatments, sampling volumes harvested for pigment, elemental, and macromolecular analyses were twofold larger than those under the other treatments.

Elemental analyses

To remove HEPES from the filters under the pH and CO_2 treatments, POC samples were rinsed three times with 30 mL of ASW (no nutrients added) with the same carbonate chemistry as in the treatment and without HEPES buffer. For POC and PON, samples were fumed with HCl for 12 h to remove inorganic carbon. TPC, POC, and PON samples were dried at 60.0°C for 12 h and analyzed using a Costech CHN analyzer. PIC quota was calculated as the difference between TPC and POC quota (Fabry and Balch 2010). To remove dissolved inorganic phosphorus from the filters, POP samples were rinsed three times with 5 mL 0.17 mol L^{-1} Na_2SO_4. After that, 2 mL 0.017 mol L^{-1} $MgSO_4$ solution was added onto filters and then POP samples were dried at 90.0°C for 12 h and combusted at 500°C for 6 h to remove POC, then cooled, and extracted by hydrolysis with 0.2 mol L^{-1} HCl (Solórzano and Sharp 1980). Phosphorus concentrations were determined using the ammonium molybdate method (Chen et al. 1956) in a microplate reader (Thermo Scientific Varioskan Lux) using adenosine-5-triphosphate disodium trihydrate (ATP007, Bioshop) as a standard.

Macromolecular analyses

Carbohydrate samples were pretreated with 12.00 mol L^{-1} of sulfuric acid (H_2SO_4) in the dark for 1 h, and then diluted by Milli-Q water for a final H_2SO_4 concentration of 1.20 mol L^{-1}. After a 5 min sonication and 30 s vortexing, samples were placed in a boiling water bath (90.0°C) for 3 h (Pakulski and Benner 1992). The concentration of monosaccharide was determined at 490 nm by phenol–sulfuric reaction with D-glucose as standard (Masuko et al. 2005).

Protein and RNA samples were immediately placed into 2 mL MP Biomedical tubes (Lysing Matrix D) containing large ceramic beads after harvesting and frozen by liquid nitrogen. Samples were stored in the dark at −80.0°C. Freeze-dried protein samples were extracted by a mixture of 0.5 mL 1X protein extraction buffer composed of lithium dodecyl sulfate (73.44 mmol L^{-1}), ethylene diamine tetraacetic acid (125.00 mmol L^{-1}), Tris base (28.07 mmol L^{-1}), Tris–HCl (21.10 mmol L^{-1}), glycerol (1085.89 mmol L^{-1}), and 4-(2-aminoethyl) benzenesulfonyl fluoride hydrochloride (0.10 mmol L^{-1}). Cells were lysed 4X1 min using a FastPrep system at 6.5 m s^{-1}. Between two cycles, samples were chilled in an ice bath for 2 min to prevent protein degradation. The samples were then centrifuged at 10,000 × g for 5 min (Spectrofuge 16M labnet). Extracted protein in the supernatant was quantified using the BCA assay with bovine gamma globulin as a standard, following Ni et al. (2016).

Total RNA was extracted by using TRIzol reagent (Invitrogen) and the RNeasy Plus Mini Kit (Qiagen). Samples were resuspended in 1.2 mL TRIzol reagent (Thermo Fisher Scientific) in lysing matrix D tubes (MP Biomedicals), homogenized by a FastPrep-24 machine (MP Biomedicals, 3 cycles, 8.0 m s^{-1}, 30 s, 3 min ice-chilling at interval), followed by

centrifugation at 12,000 × g for 3 min at 4°C (Eppendorf 5430R). RNA was extracted using a standard phenol-chloroform method (Chomczynski and Sacchi 1987). The aqueous phase was transferred to a gDNA eliminator column (from a RNeasy Plus Mini Kit) to remove the gDNA according to the manufacturer's protocol. RNA was purified by RNeasy Plus Mini Kit according to the manufacturer's protocol. Qiagen's RNase free DNase Set (an on column treatment) was further applied to remove contaminating genomic DNA according to the manufacturer's protocol. RNA was eluted into 40 μL RNase-free water, and its quality and content were analyzed using a microplate reader (Thermo Scientific Varioskan Lux). All RNA samples were tested for quality (A260/A280: 2.05–2.23; A260/A230: 2.10–2.57) (Sambrook et al. 1989).

Data analysis

ANOVA and Tukey post hoc tests were used to identify significant differences among three levels in each environmental factor (two levels for each of the light, temperature, pH, and CO_2 treatments, plus a common control for all treatments) for each of growth rate and the elemental and macromolecular ratios. Normality of residuals was checked using a Shapiro–Wilk test and a Levene test was conducted graphically to test for homogeneity of variances. A generalized least squares model was used to stabilize heterogeneity if variance was non-homogeneous. We described the relationship between measured parameters and growth rate as linear when the correlation coefficient (r) was larger than 0.80 in each environmental factor. The linear fitting and all statistical calculations were performed using R (R Core Team 2018) with the packages carData, lattice, and nlme.

Results

Elemental stoichiometry as a function of growth rate under different environmental conditions

Growth rates reduced to approximately $\frac{3}{4}\mu_{max}$ and $\frac{1}{2}\mu_{max}$ at the intermediate and low levels of light, temperature, pH, and CO_2, respectively, compared to the control (Fig. S1; Tables S2, S4). There is no universal pattern in elemental stoichiometry with growth rate (Fig. 1). PIC : POC is highest when growth rates are highest, and decreases with decreasing growth rates in each of the treatments (Fig. 1a). Except for the pH and CO_2 treatments, the shape and degree of change in PIC : POC with growth rate varies across the environmental treatments (Fig. 1a). C : N decreases linearly with decreasing growth rate in the light treatment ($r = 0.98$, $F = 195.50$, $p < 0.01$; Table S3), varies little with growth rate in the temperature treatment, and exhibits decreases in the pH and CO_2 treatments (Fig. 1b; Table S3). Both C : P and N : P increase with decreasing growth rate under the light treatment (both $r < −0.83$, $F > 22.92$, $p < 0.01$) but decrease similarly with decreasing growth rate in the temperature, pH and CO_2 treatments (all $r > 0.89$, $F > 38.02$, $p < 0.01$; Fig. 1c,d; Table S3).
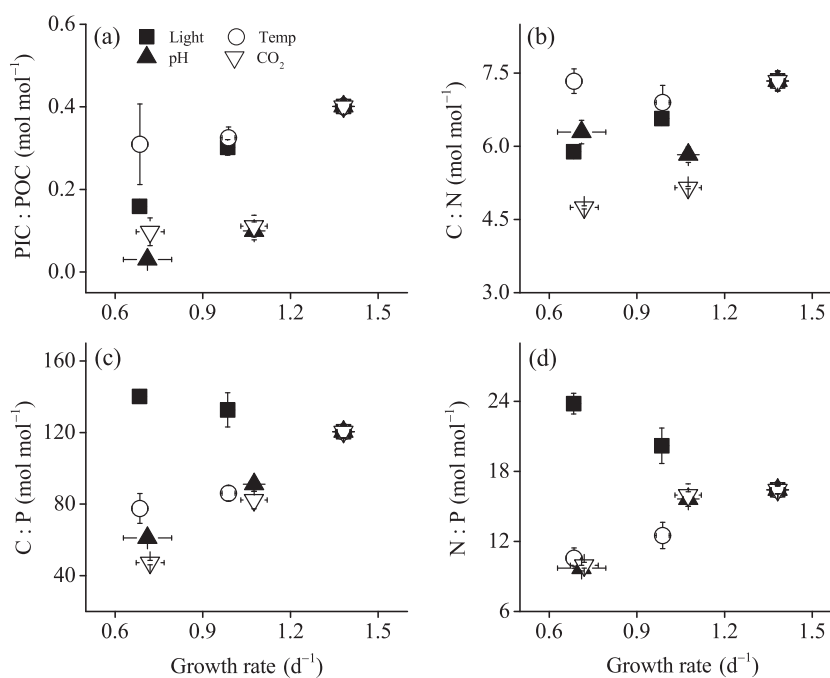
Fig. 1. The ratios of PIC : POC (**a**), C : N (**b**), C : P (**c**), and N : P (**d**) of *E. huxleyi* RCC1266 as a function of growth rate stimulated by a range of light, temperature (Temp), pH, and CO_2 conditions. Each point indicates mean $\pm$ SD of four replicates.

Macromolecular allocation as a function of growth rate under different environmental conditions

There are large differences in macromolecular allocation with growth rate across the light, temperature, pH, and CO_2 treatments (Fig. 2). In the light and CO_2 treatments, carbohydrate : POC decreases linearly with decreasing growth rates (both $r > 0.92$, $F > 54.17$, $p < 0.01$; Fig. 2a; Table S3). In contrast, under the temperature and pH treatments, carbohydrate : POC declines moderately at $^3/_4\mu_{max}$ relative to $^1/_2\mu_{max}$ or μ_{max}. Protein : POC does not change significantly with growth rate under the light treatment (Tukey HSD, $F = 3.62$, $p > 0.05$; Fig. 2b; Table S2), but under the
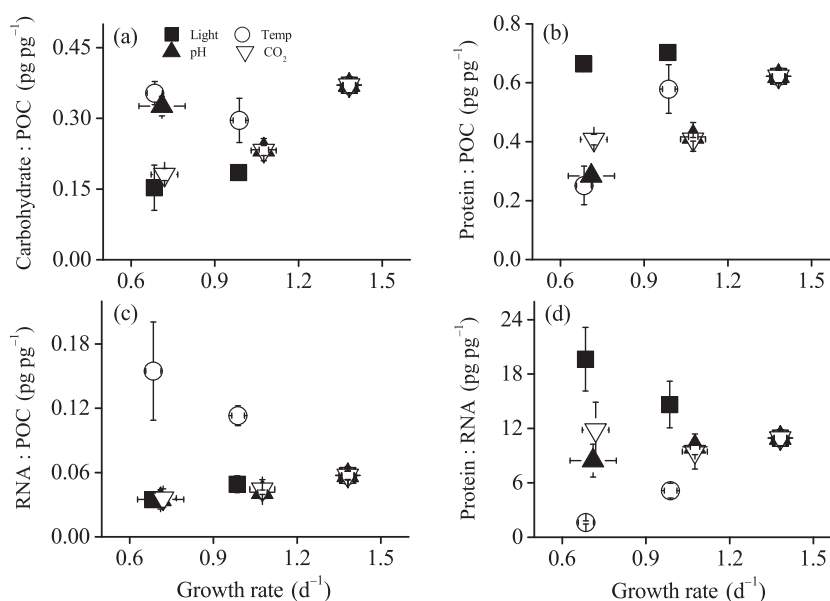

Fig. 2. Particulate organic carbon (POC) normalized carbohydrate (**a**), protein (**b**), and RNA (**c**), and protein : RNA (**d**) of *E. huxleyi* RCC1266 as a function of growth rate under the light, temperature (Temp), pH, and CO_2 treatments. Each point indicates mean $\pm$ SD of four replicates.

temperature treatment it decreases significantly between $\frac{3}{4}\mu_{max}$ and $\frac{1}{2}\mu_{max}$, while it is insignificantly different between μ_{max} and $\frac{3}{4}\mu_{max}$ (Table S2). Protein : POC appears to decrease linearly with decreasing growth rate in the temperature, pH, and CO_2 treatments ($r = 0.88$, $F = 23.68$, $p < 0.01$), although protein : POC is not significantly different between the $\frac{3}{4}\mu_{max}$ and $\frac{1}{2}\mu_{max}$ under the CO_2 treatment (Fig. 2b; Fig. S7h; Table S2). RNA : POC decreases linearly with decreasing growth rate in a very similar manner under the light, pH and CO_2 treatments (all $r > 0.83$, $F > 22.63$, $p < 0.01$; Fig. 2c; Table S3). In contrast, RNA : POC increases linearly with decreasing growth rates in the temperature treatment ($r = -0.84$, $F = 24.71$, $p < 0.01$; Fig. 2c; Table S3). Protein : RNA increases with decreasing growth rate in the light treatment, decreases with decreasing growth rates in the temperature treatment, and shows no significant change with growth rate under the pH or CO_2 treatments (Fig. 2d; Table S2).

Discussion

The GRH provides a mechanistic basis for modeling changes in macromolecular content and elemental composition (Elser et al. 2000, 2003; Inomura et al. 2020). Evidence supporting the GRH in phytoplankton is mixed. Here, we show that growth rate-associated RNA, protein, and carbon allocation strategies in *E. huxleyi* RCC1266 vary under different environmental conditions, but that physiological acclimation to specific conditions can, in part, explain deviations from the GRH and patterns in C : N : P. In this work, we compared RNA : POC and protein : POC allocation strategies and C : N : P under four different conditions (irradiance, temperature, pH, and CO_2) which were calibrated to reduce growth rate to about half and three-quarters of the maximum growth rate achieved in the control. RNA : POC and protein : POC increases with growth rate, for most but not all conditions (Fig. 2). Resource allocation to RNA and protein pools, and the resulting elemental ratios are linked to growth rate as predicted by the GRH, but the trends are modified by the effects of temperature on macromolecular synthesis rates and by the modulation of light, pH and CO_2 on protein requirements and carbon availability (Yvon-Durocher et al. 2015; Moreno and Martiny 2018). Below we discuss how physiological acclimation to temperature, irradiance, carbon limitation, and pH homeostasis can explain deviations in macromolecular and elemental composition relative to the expectations associated with the GRH (Figs. 1, 2).

Protein synthesis efficiency can be temperature sensitive, therefore the inverse relationship between cellular RNA content and RNA : POC with growth rate under the temperature treatment (Fig. 2c; Fig. S6j) likely indicates that *E. huxleyi* RCC1266 compensates for low temperature-induced decreases in protein synthesis efficiency by increasing ribosome content (Toseland et al. 2013; Schaum et al. 2018). Increases in RNA or

ribosome content under lower temperatures have been reported in the diatoms *Fragilariopsis cylindrus* and *Thalassiosira pseudonana* and there is some indication that this may occur in phytoplankton populations in the field (Toseland et al. 2013). The high RNA : POC under low growth rates in the low temperature treatment does not completely translate into low C : P or N : P (Figs. 1c,d, 2c). In *E. huxleyi* the relationship between RNA, cellular phosphorus or C : P with growth rate is complicated by condition-specific changes in intracellular phosphorus pools (Dyhrman 2016; Fig. 1c; Figs. S3m–p, S6i–l). RNA content typically contributes less than 40% of total organic phosphorus in *E. huxleyi* (Fig. S8m–p), and therefore other large pools such as polyphosphates can obscure the influence of RNA on C : P and N : P in *E. huxleyi* and other phytoplankton (Dyhrman et al. 2006; Nishikawa et al. 2006; Orchard et al. 2010).

Higher growth rates might be expected to require a higher protein : POC (Sterner and Elser 2002). Here, we find that protein : POC increases with temperature-, pH-, and CO_2-controlled increases in growth rate, but shows little change with light-induced increases in growth rate (Fig. 2b). The relatively elevated protein : POC under the two lower irradiance (28 and 45 μmol photons m^{-1} s^{-1}) treatments likely reflects an increased investment in pigment-protein complexes to increase light harvesting, and increased respiratory costs associated with their synthesis (cellular Chl *a* increases > twofold under these low irradiances (Fig. S2a)) (McKew et al. 2013). In *E. huxleyi*, and many other phytoplankton, higher light intensities are associated with lower pigment content, reducing the amount of light-induced photosystem II damage (Rokitta and Rost 2012; Li et al. 2021), and enhanced organic carbon storage in the form of carbohydrate (Fig. 2a) and lipid (Fernández et al. 1996). As a consequence, acclimation to higher irradiance is associated with elevated C : N and depressed N : P and protein : POC (Figs. 1b,d, 2b). The different patterns in protein : RNA as a function of growth rate across the environmental conditions examined are a consequence of distinct patterns in protein : POC and RNA : POC associated with acclimation to subsaturating irradiances and temperatures (Fig. 2). These results indicate that the relationship predicted by the GRH between protein : RNA and growth rate is modified by the physiological consequences of acclimation to environmental conditions.

Coccolithophores have an additional set of physiological changes induced by pH and CO_2 treatments due to calcification (Taylor et al. 2017) that can influence elemental and macromolecular composition. Both protein : POC and RNA : POC increase with growth rate across the pH and CO_2 treatments, resulting in no significant change in protein : RNA or N : P with growth rate in these treatments (Figs. 1d, 2d). In contrast, the pH and CO_2 treatments have different impacts on carbon allocation between POC and PIC (Figs. S3; Table S4). *E. huxleyi* acclimates to low CO_2 by lowering cellular Chl *a*, POC, and carbohydrate content (Table S4) and carbohydrate : POC

(Fig. 2a) and increasing carotenoid: Chl *a*. All these changes are indicative of inorganic carbon limitation of growth. Furthermore, *E. huxleyi* allocates more POC to protein synthesis and less to carbohydrate synthesis, leading to lower POC : PON and POC : POP (Fig. 1; Fig. S8d,h). POC synthesis is relatively more depressed under low CO_2 concentrations relative to the lowest pH conditions (Bach et al. 2013; Feng et al. 2018; Fig. S3g,h). Under the lowest pH treatment (highest H^+ concentration), cellular POC and carbohydrate content increased > twofold, in comparison to the control (Figs. S3g, S6c). These results indicate that H^+-driven inhibition in calcification may facilitate increased POC synthesis (Taylor et al. 2011). In other words, H^+-driven increases in CO_2 uptake may compensate for DIC limitation for organic carbon fixation or carbohydrate synthesis (Rokitta et al. 2012; Kottmeier et al. 2016). Increases in POC content under pH 7.10 vs. pH 8.05 conditions has been reported in the diatom *Skeletonema costatum* (Thoresen et al. 1984).

The C : N : P of phytoplankton influences the biogeochemical cycling of these elements (Moreno and Martiny 2018). Traditionally ecosystem models use an invariant Redfield stoichiometry for modeling C : N : P. In recent years, modeling frameworks have been introduced to better understand and incorporate variable C : N : P (Daines et al. 2014). The next-generation ocean biogeochemical models require a better quantification of differences in C : N : P across major phytoplankton function types and across species within these groups under different environmental conditions (Daines et al. 2014; Yvon-Durocher et al. 2015; Inomura et al. 2020). Although the GRH does not strictly apply to *E. huxleyi*, there are clear patterns in how macromolecular and elemental compositions vary with growth rate under different environmental conditions that can be used to model the biogeochemical impacts of coccolithophores. Although much more work is required to examine a wider range of conditions and taxa, and examine interactions among changes in multiple conditions, we expect that incorporating acclimation strategies into phytoplankton growth models will improve our ability to model broad-scale patterns in ocean biogeochemistry.

References

Arrigo, K. R. 2005. Marine microorganisms and global nutrient cycle. Nature **437**: 349–355. doi:10.1038/nature04159

Bach, L. T., L. C. M. Mackinder, K. G. Schulz, G. Wheeler, D. C. Schroeder, C. Brownlee, and U. Riebesell. 2013. Dissecting the impact of CO_2 and pH on the mechanisms of photosynthesis and calcification in the coccolithophore *Emiliania huxleyi*. New Phytol. **199**: 121–134. doi:10.1111/nph.12225

Berges, J. A., D. J. Franklin, and P. J. Harrison. 2001. Evolution of an artificial seawater medium: Improvements in enriched seawater, artificial water over the past two decades. J. Phycol. **37**: 1138–1145. doi:10.1046/j.1529-8817.2001.01052.x

Broecker, W., and E. Clark. 2009. Ratio of coccolith $CaCO_3$ to foraminifera $CaCO_3$ in late Holocene deep sea sediments. Paleoceanography **24**: PA3205. doi:10.1029/2009PA001731

Chen, P., T. T. Toribara, and H. Warner. 1956. Microdetermination of phosphorus. Anal. Chem. **28**: 1756–1758. doi:10.1021/ac60068a036

Chomczynski, P., and N. Sacchi. 1987. Single-step method of RNA isolation by acid guanidinium thiocyanate-phenol-chloroform extraction. Anal. Biochem. **162**: 156–159. doi:10.1006/abio.1987.9999

Daines, S. J., J. R. Clark, and T. M. Lenton. 2014. Multiple environmental controls on phytoplankton growth strategies determine adaptive responses of the N:P ratio. Ecol. Lett. **17**: 414–425. doi:10.1111/ele.12239

Diaz, J. M., K. M. Björkman, S. T. Haley, E. D. Ingall, D. M. Karl, A. F. Longo, and S. T. Dyhrman. 2016. Polyphosphate dynamics at station ALOHA, North Pacific subtropical gyre. Limnol. Oceanogr. **61**: 227–239. doi:10.1002/lno.10206

Dickson, A. G., C. L. Sabine, and J. R. Christian. 2007. Guide to best practice for ocean CO2 measurements. PICES Special Publicaiton 3, 191 pp.

Dyhrman, S. T. 2016. Nutrients and their acquisition: Phosphorus physiology in microalgae. p. 155–183. *In* M. A. Borowitzka, J. Beardall, and J. A. Raven [eds.], The physiology of microalgae. Heidelberg, Germany, Springer. doi: 10.1007/978-3-319-24945-2

Dyhrman, S. T., S. T. Haley, S. R. Birkeland, L. L. Wurch, M. J. Cipriano, and A. G. McArthur. 2006. Long serial analysis of gene expression for gene discovery and transcriptome profiling in the widespread marine coccolithophore *Emiliania huxleyi*. Appl. Environ. Microb. **72**: 252–260. doi:10.1128/AEM.72.1.252-260.2006

Elser, J. J., and others. 2003. Growth rate–stoichiometry couplings in diverse biota. Ecol. Lett. **6**: 936–943. doi:10.1046/j.1461-0248.2003.00518.x

Elser, J. J., and others. 2000. Biological stoichiometry from genes to ecosystems. Ecol. Lett. **3**: 540–550. doi:10.1111/j.1461-0248.2000.00185.x

Engel, A., C. C. Novoa, M. Wurst, S. Endres, T. Tang, M. Schartau, and C. Lee. 2014. No detectable effect of CO_2 on elemental stoichiometry of *Emiliania huxleyi* in nutrient-limited, acclimated continuous cultures. Mar. Ecol. Prog. Ser. **507**: 15–30. doi:10.3354/meps10824

Fabry, V. J., and W. M. Balch. 2010. Direct measurements of calcification rates in planktonic organisms, p. 201–212. *In* U. Riebesell, V. J. Fabry, L. Hansson, and J. P. Gattuso [eds.], Guide to best practices for ocean acidification research and data reporting. Luxembourg: Publications Office of the European Union. doi:10.2777/66906

Feng, Y. Y., M. Y. Roleda, E. Armstrong, C. S. Law, P. W. Boyd, and C. L. Hurd. 2018. Environmental controls on the elemental composition of a Southern Hemisphere strain of

the coccolithophore *Emiliania huxleyi*. Biogeosciences **15**: 581–595. doi:10.5194/bg-15-581-2018

Fernández, E., J. J. Fritz, and W. M. Balch. 1996. Chemical composition of the coccolithophorid *Emiliania huxleyi* under light-limited steady state growth. J. Exp. Mar. Biol. Ecol. **207**: 149–160. doi:10.1016/S0022-0981(96)02657-3

Finkel, Z. V., M. J. Follows, J. D. Liefer, C. M. Brown, I. Benner, and A. J. Irwin. 2016. Phylogenetic diversity in the macromolecular composition of microalgae. PLoS One **11**: e0155977. doi:10.1371/journal.pone.0155977

Finkel, Z., J. Beardall, K. J. Flynn, A. Quigg, T. A. V. Rees, and J. A. Raven. 2010. Phytoplankton in a changing world: Cell size and elemental stoichiometry. J. Plankton Res. **32**: 119–137. doi:10.1093/plankt/fbp098

Flynn, K. J., J. A. Raven, T. A. V. Rees, Z. Finkel, A. Quigg, and J. Beardall. 2010. Is the growth rate hypothesis applicable to microalgae? J. Phycol. **46**: 1–12. doi:10.1111/j.1529-8817.2009.00756.x

Garcia, N. S., J. A. Bonachela, and A. C. Martiny. 2016. Inter-actions between growth-dependent changes in cell size, nutrient supply and cellular elemental stoichiometry of marine Synechococcus. ISME J. **10**: 2715–2724. doi:10.1038/ismej.2016.50

Giordano, M., M. Palmucci, and J. A. Raven. 2015. Growth rate hypothesis and efficiency of protein synthesis under different sulphate concentrations in two green algae. Plant Cell Environ. **38**: 2313–2317. doi:10.1111/pce.12551

Guillard, R. R. L., and J. H. Ryther. 1962. Studies of marine planktonic diatoms. I. *Cyclotella nana* Hustedt and *Detonula confervacea* Cleve. Can. J. Microbiol. **8**: 229–239. doi:10.1139/m62-029

Guillard, R. R. L., and P. E. Hargraves. 1993. *Stichochrysis immobilis* is a diatom, not a chrysophyte. Phycologia **32**: 234–236. doi:10.2216/i0031-8884-32-3-234.1

Harris, G. N., D. J. Scanlan, and R. J. Geider. 2009. Responses of *Emiliania huxleyi* (Prymnesiophyceae) to step changes in photon flux density. Eur. J. Phycol. **44**: 31–48. doi:10.1080/09670260802233460

Hinga, K. R. 2002. Effects of pH on coastal marine phyto-plankton. Mar. Ecol. Prog. Ser. **238**: 281–300. doi:10.3354/meps238281

Iida, T., K. Mizobata, and S. I. Saitoh. 2012. Interannual vari-ability of coccolithophore *Emiliania huxleyi* blooms in response to changes in water column stability in the east-ern Bering Sea. Cont. Shelf Res. **34**: 7–17. doi:10.1016/j.csr.2011.11.007

Inomura, K., A. W. Omta, D. Talmy, J. Bragg, C. Deutsch, and M. J. Follows. 2020. A mechanistic model of macromolec-ular allocation, elemental stoichiometry, and growth rate in phytoplankton. Front. Microbiol. **11**: 86. doi:10.3389/fmicb.2020.00086

Jin, P., J. C. Ding, T. Xing, U. Riebesell, and K. S. Gao. 2017. High levels of solar radiation offset impacts of ocean acidifi-cation on calcifying and non-calcifying strains of *Emiliania*

huxleyi. Mar. Ecol. Prog. Ser. **568**: 47–58. doi:10.3354/meps12042

Kondrik, D., E. Kazakov, and D. Pozdnyakov. 2019. A syn-thetic satellite dataset of the spatio-temporal distributions of *Emiliania huxleyi* blooms and their impacts on Arctic and sub-Arctic marine environments (1998-2016). Earth Syst. Sci. Data **11**: 119–128. doi:10.5194/essd-11-119-2019

Kottmeier, D. M., S. D. Rokitta, and B. Rost. 2016. H^+-driven increase in CO_2 uptake and decrease in HCO_3^- uptake explain coccolithophores' acclimation responses to ocean acidification. Limnol. Oceanogr. **61**: 2045–2057. doi:10.1002/lno.10352

Krumhardt, K. M., N. S. Lovenduski, M. D. Iglesias-Rodriguez, and J. A. Kleypas. 2017. Coccolithophore growth and calci-fication in a changing ocean. Prog. Oceanogr. **171**: 276–295. doi:10.1016/j.pocean.2017.10.007

Leonardos, K., and R. J. Geider. 2005. Elevated atmospheric carbon dioxide increases organic carbon fixation by *Emiliania huxleyi* (haptophyta), under nutrient-limited high-light conditions. J. Phycol. **41**: 1196–1203. doi:10.1111/j.1529-8817.2005.00152.x

Li, Z., W. Li, Y. Zhang, Y. Hu, R. Sheward, A. J. Irwin, and Z. V. Finkel. 2021. Dynamic photophysiological stress response of a model diatom to ten environmental stresses. J. Phycol. **57**: 484–495. doi:10.1111/jpy.13072-20-099

Liefer, J. D., A. Garg, M. H. Fyfe, A. J. Irwin, I. Benner, C. M. Brown, M. J. Follows, A. W. Omta, and Z. V. Finkel. 2019. The macromolecular basis of phytoplankton C:N:P under nitrogen starvation. Front. Microbiol. **10**: 763. doi:10.3389/fmicb.2019.00763

Martiny, A. C., and others. 2016. Biogeochemical interactions control a temporal succession in the elemental composition of marine communities. Limnol. Oceanogr. **61**: 531–542. doi:10.1002/lno.10233

Martiny, A. C., C. T. A. Pham, F. W. Primeau, J. A. Vrugt, J. K. Moore, S. A. Levin, and M. W. Lomas. 2013. Strong latitudi-nal patterns in the elemental ratios of marine plankton and organic matter. Nature Geosci. **6**: 279–283. doi:10.1038/NGEO1757

Masuko, T., A. Minami, N. Iwasaki, T. Majima, S. I. Nishimura, and Y. C. Lee. 2005. Carbohydrate analysis by a phenol-sulfuric acid method in microplate format. Anal. Biochem. **339**: 69–72. doi:10.1016/j.ab.2004.12.001

McKew, B. A., and others. 2013. The trade-off between the light-harvesting and photoprotective functions of fucoxanthin-chlorophyll proteins dominates light acclimation in *Emiliania huxleyi* (clone CCMP 1516). New Phytol. **200**: 74–85. doi:10.1111/nph.12373

Moreno, A. R., and A. C. Martiny. 2018. Ecological stoichiom-etry of ocean plankton. Ann. Rev. Mar. Sci. **10**: 43–69. doi:10.1146/annurev-marine-121916-063126

Ni, G., G. Zimbalatti, C. D. Murphy, A. B. Barnett, C. M. Arsenault, G. Li, A. M. Cockshutt, and D. A. Campbell. 2016. Arctic *Micromonas* uses protein pools and non-photochemical

quenching to cope with temperature restrictions on photo-system II protein turnover. Photosynth. Res. **131**: 203–220. doi:10.1007/s11120-016-0310-6

Nicklisch, A., and C. E. W. Steinberg. 2009. RNA/protein and RNA/DNA ratios determined by flow cytometry and their relationship to growth limitation of selected planktonic algae in culture. Eur. J. Phycol. **44**: 297–308. doi:10.1080/09670260802578518

Nishikawa, K., H. Machida, Y. Yamakoshi, R. Ohtomo, K. Saito, M. Saito, and N. Tominaga. 2006. Polyphosphate metabolism in an acidophilic alga *Chlamydomonas acidophila* KT-1 (Chlorophyta) under phosphate stress. Plant Sci. **170**: 307–313. doi:10.1016/j.plantsci.2005.08.025

Olson, M. B., T. A. Wuori, B. A. Love, and S. L. Strom. 2017. Ocean acidification effects on haploid and diploid *Emiliania huxleyi* strains: Why changes in cell size matter. J. Exp. Mar. Biol. Ecol. **488**: 72–82. doi:10.1016/j.jembe.2016.12.008

Orchard, E. D., J. W. Ammerman, M. W. Lomas, and S. T. Dyhrman. 2010. Dissolved inorganic and organic phosphorus uptake in *Trichodesmium* and the microbial community: The importance of phosphorus ester in the Sargasso Sea. Limnol. Oceanogr. **55**: 1390–1399. doi:10.4319/lo.2010.55.3.1390

Pakulski, J. D., and R. Benner. 1992. An improved method for the hydrolysis and MBTH analysis of dissolved and particulate carbohydrates in seawater. Mar. Chem. **40**: 143–160. doi:10.1016/0304-4203(92)90020-B

Pierrot, D., E. Lewis, and D. W. R. Wallace. 2006. MS Excel program developed for CO_2 system calculations, ORNL/CDIAC-105, Carbon Dioxide Information Analysis Centre, Oak Ridge National Laboratory, U.S., Department of Energy.

Poulton, A. J., T. R. Adey, W. M. Balch, and P. M. Holligan. 2007. Relating coccolithophore calcifcation rates to phytoplankton community dynamics: Regional diferences and implications for carbon export. Deep Sea Res. Part II **54**: 538–557. doi:10.1016/j.dsr2.2006.12.003

R Core Team. 2018. The R foundation for statistical computing platform. x86_64-w64-mingw32/x64. Available from: https://cran.r-project.org/bin/windows/base/old/3.5.0.

Redfield, A. C. 1958. The biological control of the chemical factors in the environment. Am. Sci. **46**: 205–221. doi:10.1086/646891

Riebesell, U., and P. D. Tortell. 2011. Effects of ocean acidification on pelagic organisms and ecosystems, p. 99–121. *In* J. P. Gattuso and L. Hansson [eds.], Ocean acidification. Oxford Univ. Press.

Rivero-Calle, S., A. Gnanadesikan, C. E. Del Castillo, W. M. Balch, and S. D. Guikema. 2015. Multidecadal increase in North Atlantic coccolithophores and the potential role of rising CO_2. Science **350**: 1533–1537. doi:10.1126/science.aaa8026

Rokitta, S. D., and B. Rost. 2012. Effects of CO_2 and their modulation by light in the life-cycle stages of the coccolithophore *Emiliania huxleyi*. Limnol. Oceanog. **57**: 607–618. doi:10.4319/lo.2012.57.2.0607

Rokitta, S. D., U. John, and B. Rost. 2012. Ocean acidification affects redox-balance and ion-homeostasis in the life-cycle stages of *Emiliania huxleyi*. PLoS One **7**: e52212. doi:10.1371/journal.pone.005221

Rost, B., and U. Riebesell. 2004. Coccolithophores and the biological pump: Responses to environmental changes, p. 99–125. *In* H. R. Thierstein and J. Young [eds.], Coccolithophores: From molecular biology to global impact. Springer.

Roy, R. N., L. N. Roy, K. M. Vogel, C. Porter-Moore, T. Pearson, C. E. Good, F. J. Millero, and D. C. Campbell. 1993. Thermodynamics of the dissociation of boric acid in seawater at S 5 35 from 0 degrees C to 55 degrees C. Mar. Chem. **44**: 243–248. doi:10.1016/0304-4203(93)90206-4

Sambrook, J., E. F. Fritsch, and T. Maniatis. 1989. Molecular cloning: A laboratory manual, 2nd ed. Cold Spring Harbor, New York: Cold Spring Harbor Laboratory Press.

Schaum, C. E., A. Buckling, N. Smirnoff, D. J. Studholme, and G. Yvon-Durocher. 2018. Environmental fluctuations accelerate molecular evolution of thermal tolerance in a marine diatom. Nat. Commun. **9**: 1719. doi:10.1038/s41467-018-03906-5

Solórzano, L., and J. H. Sharp. 1980. Determination of total dissolved phosphorus and particulate phosphorus in nature waters. Limnol. Oceanogr. **25**: 754–758. doi:10.4319/lo.1980.25.4.0754

Sterner, R. W., and J. J. Elser. 2002. Ecological stoichiometry: The biology of elements from molecules to the biosphere. Princeton: Princeton Univ. Press.

Taylor, A. R., A. Chrachri, G. Wheeler, H. Goddard, and C. Brownlee. 2011. A voltage-gated H^+ channel underlying pH homeostasis in calcifying coccolithophores. PLoS Biol. **9**: e1001085. doi:10.1371/journal.pbio.1001085

Taylor, A. R., C. Brownlee, and G. Wheeler. 2017. Coccolithophore cell biology: Chalking up progress. Ann. Rev. Mar. Sci. **9**: 283–310. doi:10.1146/annurev-marine-122414-034032

Thoresen, S. S., J. R. Clayton, and S. I. Ahmed. 1984. The effect of short-term fluctuations in pH on NO_3^- uptake and intracellular constituents in *Skeletonema costatum* (Grev.) cleve. J. Exp. Mar. Biol. Ecol. **83**: 149–157. doi:10.1016/0022-0981(84)90042-x

Toseland, A., and others. 2013. The impact of temperature on marine phytoplankton resource allocation and metabolism. Nat Clim. Change **3**: 979–984. doi:10.1038/NCLIMATE1989

Wang, X., F. Fu, P. Qu, J. D. Kling, H. Jiang, Y. Gao, and D. A. Hutchins. 2019. How will the key marine calcifier *Emiliania huxleyi* respond to a warmer and more thermally variable ocean? Biogeosciences **16**: 4393–4409. doi:10.5194/bg-2019-179

Weber, T. S., and C. Deutsch. 2010. Ocean nutrient ratios governed by plankton biogeography. Nature **467**: 550–554. doi:10.1038/nature09403

Yvon-Durocher, G., M. Dossena, M. Trimmer, G. Woodward, and A. P. Allen. 2015. Temperature and the biogeography of algal stoichiometry. Glob. Ecol. Biogeogr. **24**: 562–570. doi:10.1111/geb.12280

Conflict of Interest

The authors declared that they have no conflicts of interest.